Applied Catalysis B: Environmental 160–161 (2014) 80–88

Contents lists available at ScienceDirect

Applied Catalysis B: Environmental

journal homepage: www.elsevier.com/locate/apcatb

Oxidation of organosulfur compounds using an iron(III) porphyrin complex: An environmentally safe and efficient approach

Sónia M.G. Pires[a], Mário M.Q. Simões[a,*], Isabel C.M.S. Santos[a], Susana L.H. Rebelo[b], Filipe A. Almeida Paz[c], M. Graça P.M.S. Neves[a,*], José A.S. Cavaleiro[a]

[a] QOPNA, Department of Chemistry, University of Aveiro, 3810-193 Aveiro, Portugal
[b] REQUIMTE, Department of Chemistry and Biochemistry, Faculty of Sciences, University of Porto, Rua do Campo Alegre, 4169-007 Porto, Portugal
[c] CICECO, Department of Chemistry, University of Aveiro, 3810-193 Aveiro, Portugal

ARTICLE INFO

Article history:
Received 16 January 2014
Received in revised form 24 April 2014
Accepted 3 May 2014
Available online 14 May 2014

Keywords:
Iron
Porphyrins
Oxidation
Organosulfur compounds
Hydrogen peroxide

ABSTRACT

Following our approach on the use of metalloporphyrins as catalysts and hydrogen peroxide as oxidant in the oxidation of organosulfur compounds (e.g. sulfides, benzothiophenes and dibenzothiophenes), herein the excellent catalytic performance of a homogeneous iron(III) porphyrin complex is demonstrated. Beyond the better results obtained, when compared with those with manganese(III) complexes, the present procedure involves a cleaner approach because ethanol is used as solvent and a co-catalyst is not required. For all the studied substrates (**1**–**10**), conversions higher than 95% were achieved with $Fe(TF_4NMe_2PP)Cl$ (**I**). More significantly, catalyst (**I**) is also efficient in the oxidation of a model fuel, constituted by a mixture of benzothiophene (**3**), 3-methylbenzothiophene (**5**), 4-methyldibenzothiophene (**8**) and 4,6-diethyldibenzothiophene (**10**) in hexane, affording an overall conversion of 84%.

© 2014 Elsevier B.V. All rights reserved.

1. Introduction

Nowadays the negative impact induced by the presence of organosulfur compounds such as benzothiophenes (BTs) and dibenzothiophenes (DBTs) in fuels is well established. Beyond the SO_X emissions resulting from the combustion of organosulfur compounds, normally associated with the formation of acid rains, their presence is also responsible for the poisoning of catalysts and corrosion of internal parts of combustion engines [1–3]. Furthermore, the very restrictive regulations recently approved, limiting the sulfur content on petroleum products, allied to the technical limitations of the common hydrodesulphurization procedures (HDS), boosted an intense research in the area, and therefore the appearance of very promising and much more environmentally sustainable alternatives such as the oxidative desulfurization (ODS) or the biodesulfurization (BDS) methodologies [4–7].

It is important to understand that, to meet the new regulations, HDS involves at present significant costs for refineries, associated either to the consumption of hydrogen or to the higher temperatures and pressures essential for deep desulfurization. Moreover, and contrasting with ODS and BDS, HDS can not readily achieve the very low sulfur levels envisaged for future "zero sulfur" contents [8,9]. From an economical point of view, it has been already proven that BDS is hardly viable at an industrial scale; on the other hand, ODS presents recognized advantages such as the lower capital and operating costs needed to be integrated in the already hydrotreating units [1,4]. So, much attention has been given to the development of new ODS methodologies using distinct types of catalysts, homogeneous or heterogeneous, organic or inorganic, and involving the use of a wide range of oxidants (*t*-butyl hydroperoxide, cumene hydroperoxide, PhIO, O_3, O_2, among others), being H_2O_2 the most commonly used both by efficiency and environmental protection reasons [10,11]. Besides, the synthesis of sulfoxides/sulfones constitute an important methodology in organic chemistry, useful in the synthesis of natural products and biological active molecules [12–15].

In biological systems, the main responsible for the selective production of sulfoxides, sulfones, and even chiral sulfoxides are the cytochrome P450 monooxygenases, which are able to catalyze sulfoxidations under very mild conditions, as well as several other oxidative transformations [16–19]. These enzymes present in their active site the iron complex of protoporphyrin IX. With the objective of mimicking their extraordinary catalytic activity, in 1979

* Corresponding authors at: QOPNA, Department of Chemistry, University of Aveiro, 3810-193 Aveiro, Portugal. Tel.: +351234370713/+351234370710; fax: +351234370084.
E-mail addresses: msimoes@ua.pt (M.M.Q. Simões), gneves@ua.pt (M.G.P.M.S. Neves).

http://dx.doi.org/10.1016/j.apcatb.2014.05.003
0926-3373/© 2014 Elsevier B.V. All rights reserved.

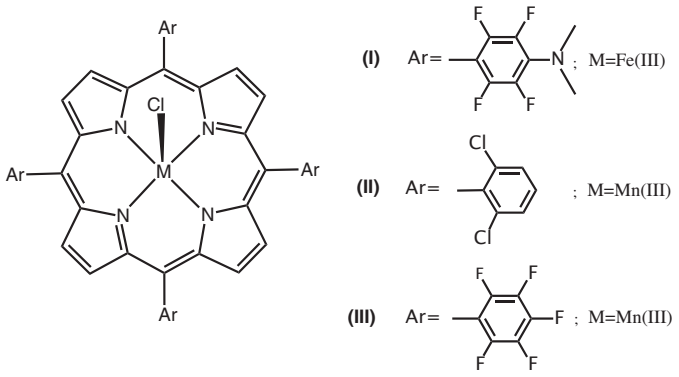
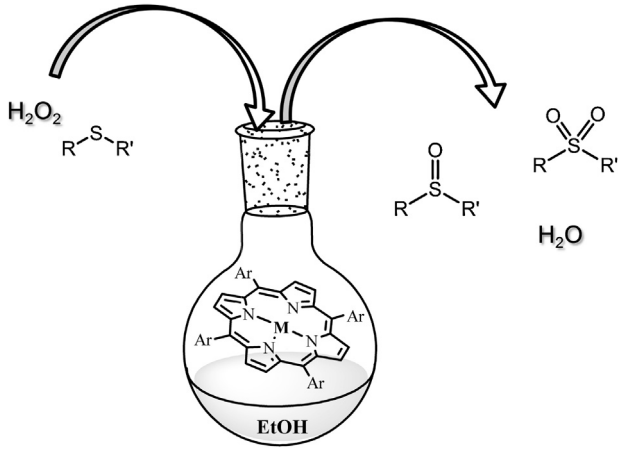


Fig. 1. Metalloporphyrins studied as catalysts.



Scheme 1.

Groves reported for the first time the use of a metalloporphyrin (MPorph)-based catalytic system for alkene epoxidation [20]. Since then MPorph-based catalytic systems have been successfully used as biomimetic models of cytochrome P450s triggering the interest of several research groups spread all over the world. Many improvements have been disclosed in the literature, such as the appearance of more oxidative resistant catalysts or the development of heterogeneous catalysts, namely through the immobilization on several organic/inorganic supports using a wide range of approaches [21–25].

Considering the excellent capabilities of metalloporphyrins as biomimetic models of P450s we have recently demonstrated the high efficiency of manganese(III) porphyrin catalysts in the oxidation of BTs and DBT by H_2O_2 under homogeneous conditions [26]. Comparatively to Mn(III) complexes, in the oxidations carried out in the presence of iron(III) porphyrins, different catalytic species are involved and, depending on the studied substrates, different oxidation products can be observed. Additionally, iron(III) porphyrins not only allow to perform oxidative transformations in the absence of a co-catalyst, as are also effective if protic, greener and sustainable solvents, such as ethanol or methanol, are employed [27–30]. Thus, following our interest on the search for green, and efficient oxidative desulfurization methodologies and the relevance of this research field, we are now extending the oxidative catalytic tests with different organosulfur compounds in the presence of H_2O_2 to an iron(III) complex, known for its catalytic properties. In fact, only a handful of reports considered the use of iron(III)Porph catalytic systems in the oxidation of organosulfur derivatives [31–33]. Le Maux and Simonneaux successfully performed the asymmetric oxidation of different sulfides by H_2O_2 using chiral water-soluble iron porphyrins as catalysts leading to optically active sulfoxides with ee up to 90% [32]. Also in 2011, it has been reported the use of a Fe(III) porphyrin in the direct oxygenation of two DBTs by oxygen. In this procedure, under the optimized conditions, the full conversion of DBTs into the corresponding sulfones was attained after 3 h of reaction at 120 °C and 0.5 MPa in the presence of 0.1 wt% of catalyst [33].

This report constitutes the first time that the iron(III) porphyrin complex $FeTNMe_2F_4PPCl$ (catalyst **I**, Fig. 1) is tested with a so large batch of BTs and DBTs (Fig. 2), using very moderate conditions, namely at room temperature (only one substrate required the use of heating for a better conversion under environmentally friendly conditions) and normal pressure. In order to fully establish the potential of this Fe(III)Porph catalytic system, several recalcitrant BTs and DBTs were studied, namely substituted DBTs such as 4-methyldibenzothiophene (4-MDBT) (**8**), 4,6-dimethyldibenzothiophene (4,6-DMDBT) (**10**) and 4,6-diethyldibenzothiophene (4,6-DEDBT) (**9**).

2. Results and discussion

During the last years our group gained significant expertise in the use of MPorph as catalysts in the oxyfunctionalization of alkenes [27,34], aromatic substrates [35–37], natural occurring compounds with relevant biological activity [38,39], or even drugs [40,41], under very mild conditions [42,43]. Considering the relevance of the development of new ODS methodologies, and encouraged by the promising results achieved for the oxidation of several organosulfur compounds using manganese(III) porphyrin complexes and H_2O_2 as oxidant [26], we decided to extend our approach to a different metalloporphyrin catalytic system. Under the new conditions the catalytic sulfoxidation of substrates **1–10** (Fig. 2) by H_2O_2 was performed in the presence of $FeTNMe_2F_4PPCl$ (**I**, Fig. 1) using ethanol as solvent (Scheme 1). Due to the insolubility of substrate **10** its oxidation required slightly different experimental conditions; in order to facilitate the discussion, the analysis of the results obtained with this substrate will be separated from those obtained with substrates **1**–**9**. The catalytic oxidation of these nine substrates was performed at room temperature, in the absence of light, and the oxidant being progressively added to the reaction mixture in small amounts (0.5 eq.) every 15 min. The reactions were monitored by GC-FID and the oxidant additions were stopped when no significant evolution in two successive analyses was observed.

Although the experimental procedure seems similar to that described for manganese catalysts [26], there are two important differences that must be highlighted: the solvent used in the

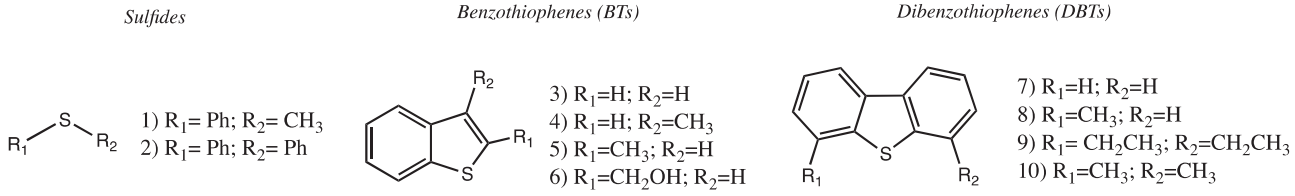


Fig. 2. Organosulfur compounds studied for sulfoxidation with H_2O_2 using metalloporphyrin catalysts.

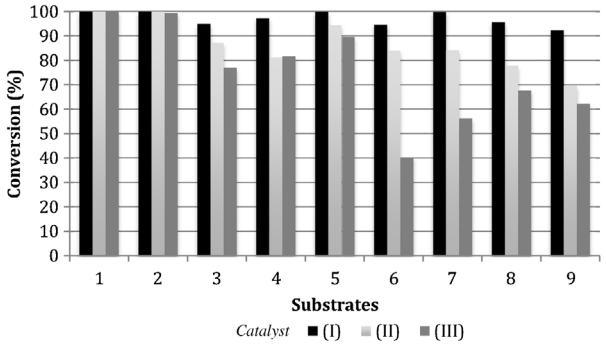


Fig. 3. Conversion values obtained for substrates **1**–**9** after 90 min of reaction in the presence of H_2O_2, using a S/C molar ratio of 300.

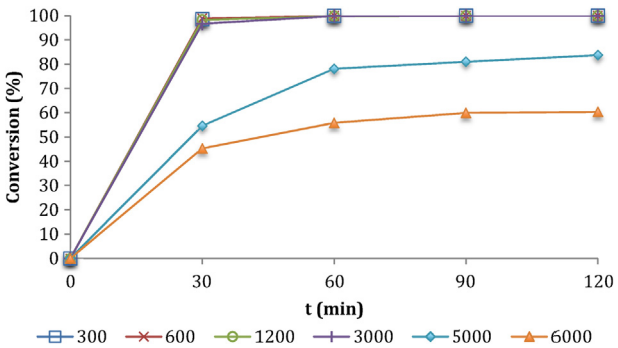


Fig. 4. Thioanisole (**1**) oxidation reaction profile in the presence of catalyst (I) using different S/C molar ratios.

reaction and in the dilution of the aqueous hydrogen peroxide, and the presence or the absence of a co-catalyst. As mentioned, for a FePorph/H_2O_2 catalytic system the formation of the hydroperoxy active species is favored by the use of a protic solvent and does not require the presence of a co-catalyst [27,44]. On the other hand, in the case of the MnPorph/H_2O_2 catalytic system, where the oxo-species is considered the main active catalytic species, its formation is favored in the presence of an aprotic solvent and of a buffering substance as the co-catalyst [27,44]. Thus, in the catalytic experiments using catalyst **I**, ethanol was the solvent of choice, and no co-catalyst was used. When catalysts **II** and **III** were involved, the solvent was CH_3CN and the co-catalyst used was ammonium acetate [45].

In Table 1 are summarized the results achieved in the catalytic assays using the iron catalyst **I** and in Table 2 those obtained in the oxidation of substrates **8** and **9** with manganese complexes **II** and **III**. For comparative purposes, the previous results obtained with catalysts **II** and **III** for substrates **1–7** are summarized in Table S1 (Supporting information) [26]. It is important to refer that the blank experiments (without catalyst) were performed for all the organosulfur compounds **1–9** and no significant conversions were observed, being lower than 5% for all cases. Catalyst **I** is the most efficient in the sulfoxidation of substrates **1–9**. Besides achieving more rapidly almost total conversion for all the organosulfur compounds studied, including the most recalcitrant DBTs (**7–9**), permits also the use of lower amounts of catalyst, without significant decrease in the efficiency. It is notable that, comparatively to the manganese porphyrin complexes, and even using a substrate/catalyst (S/C) molar ratio of 600, catalyst **I** allows conversions ranging from 88.6 to 99.9%. Fig. 3, which compares the activity of catalysts **I**–**III** after 90 min of reaction for substrates **1–9**, using a S/C molar ratio of 300, put in evidence the greater efficiency of the iron porphyrin (**I**) in the performed sulfoxidations. Conversely, with catalysts **II** and **III**, after 90 min of reaction with catalyst **I** the conversions are already higher than 90% for all cases, even for the more recalcitrant DBTs (**7–9**).

Sulfides **1** and **2** are easily oxidized by H_2O_2 in the presence of all the porphyrin catalysts (**I–III**), probably due to the fact that the sulfur unshared electrons are not involved in the aromatic system (as for BTs and DBTs). However, the extraordinary catalytic activity of the iron complex (**I**) in the oxidation of this kind of substrates deserves to be highlighted. For example, for thioanisole (**1**) it was necessary to work with at S/C molar ratio of 5000 to observe a significant decrease on catalyst **I** activity (Table 3 and Fig. 4).

At the S/C molar ratio of 3000 and despite the excellent conversion, still above 95%, the corresponding sulfone is no longer the only product observed at the end of the reaction. The sulfoxide/sulfone ratio is around 5.0 for selectivity values around 83.5% for the S=O and 16.5% for the SO_2.

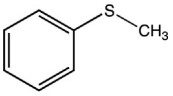
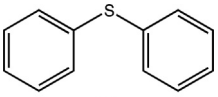
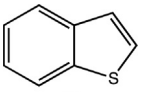
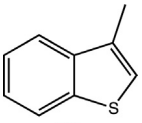
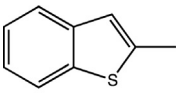
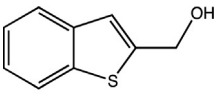
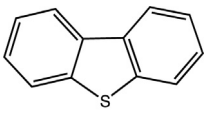
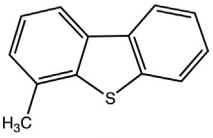
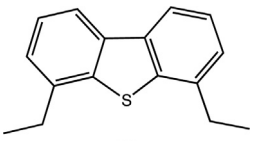
In the case of BTs (**3–6**), the reactivity seems to be affected not only by the presence of different substituents in the thiophene ring, but also by their position. For catalyst (**I**), and using a S/C molar ratio of 1200, the negative impact induced by the methyl substituent is evident in the conversion obtained (44.6%) for compound **4**; furthermore, the sulfone is no longer obtained. Nevertheless, this is not observed when the same substituent is in a different position (at position 2), and for compound **5** conversions above 90% are achieved. It is interesting to note that and comparatively to the iron complex (**I**), for manganese catalysts (**II**, **III**) this effect is not so evident (Table S1). Concerning compound **6**, both the manganese and the iron catalysts give rise to lower conversions if compared to the similar substituted compound **5**.

From the experiments with the DBTs (**7–9**), it seems relevant that the alkyl monosubstitution of one of the benzene rings, for both catalytic systems, led to similar or slightly higher conversions; thus, the increased steric hindrance does not seem to affect much the oxidation results. This is not the case of the alkyl disubstituted DBT (**9**), for which the poorer results can be attributed to the higher steric hindrance induced by the two ethyl groups near the heteroatom. In fact, for the S/C molar ratio of 1200 the conversion reaches only 43.7% and it is the only substrate that, in all assays, does not give the corresponding sulfone as the main product.

In summary, for the catalytic assays with substrates (**1–9**) and FeTNMe$_2$F$_4$PPCl (**I**), using H_2O_2, a more efficient and environmentally friendly approach was settled, as it uses ethanol as solvent and does not require the use of a co-catalyst. The superior performance of the iron catalyst can be understood through the different catalytic species involved in the two systems tested (iron and manganese) under the optimal reaction conditions. The structure/reactivity of the substrate has also an important role on the catalytic sulfoxidation reactions performed with the metalloporphyrin complexes. In the case of the iron catalyst **I**, and from the obtained results, the position and the type of substitution on the starting BT or DBT seems to have a significant effect on its reactivity toward the oxidation using hydrogen peroxide.

Considering substrate **10**, it was possible to modify the catalytic assays for manganese and iron complexes, due to its poor solubility either in CH_3CN or ethanol at room temperature. Based on the aforementioned protocol, the initial catalytic studies were performed with catalyst **II**, and the modification of some parameters such as solvent, temperature and stirring method (magnetic or by sonication) have been tested. The results from these preliminary assays are summarized in Table 4, entries 1–9). All the results have been determined after 3 h of reaction and after purification by preparative TLC. The best reaction conditions for catalyst (**II**) are shown in entry 8, when the temperature was set to 60 °C and CH_3CN was the solvent of choice; with these conditions it was possible to achieve 90.5% of conversion into the corresponding oxidation products, sulfoxide **13** (40.3%) and sulfone **14** (24.4%). The possibility

Table 1
Results obtained for the oxidation of substrates (**1**–**9**) with H_2O_2 catalyzed by the iron(III) porphyrin complex (I)[a].

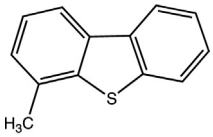
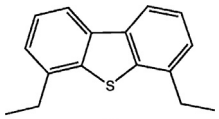
Substrates	S/C molar ratio	H_2O_2 (m mol)	Conversion (%)	Products selectivity (%)		Time (min)
				S=O	SO_2	
 (1)	300	0.6	99.9	–	100	60
	600	0.6	99.9	–	100	60
	1200	1.2	97.2	–	100	120
 (2)	300	0.9	99.9	–	100	90
	600	0.9	99.9	–	100	90
	1200	0.9	99.9	6.9	93.1	90
 (3)	300	1.2	99.9	–	100	120
	600	1.2	99.9	–	100	120
	1200	1.5	92.4	3.2	96.8	150
 (4)	300	0.9	99.9	–	100	90
	600	1.2	98.4	–	100	120
	1200	1.2	44.6	100	0	120
 (5)	300	1.5	99.9	–	100	150
	600	1.5	99.9	–	100	150
	1200	1.5	90.1	54.8	45.2	150
 (6)	300	1.8	99.5	–	100	180
	600	1.8	96.1	–	100	180
	1200	1.8	73.8	*	*	180
 (7)	300	0.9	99.9	–	100	90
	600	1.5	98.7	–	100	150
	1200	1.8	71.3	*	*	180
 (8)	300	1.5	99.7	–	100	150
	600	1.8	98.2	2.1	97.9	180
	1200	1.8	84.4	10	90	180
 (9)	300	1.8	96.3	88.5	22.9	180
	600	1.8	88.6	59.8	40.2	180
	1200	1.2	43.7	80.9	19.1	120

[a] The substrate (0.3 mmol) was dissolved in 2.0 mL of ethanol and kept under magnetic stirring at 22–25 °C in the presence of the iron(III) catalyst **I** (for the S/C molar ratio of 300, the catalyst amount was 1.0×10^{-3} mmol; for the S/C molar of 600, the catalyst amount was 0.5×10^{-3} mmol; for the S/C molar of 1200, the catalyst amount was 0.25×10^{-3} mmol). The oxidant, diluted 1:10 in ethanol, was progressively added at regular intervals of 15 min in small aliquots, each corresponding to a half-substrate amount. The conversion and selectivity values are the result of at least two essays.
* The chromatograms do not allow the determination of the corresponding selectivity.

of using solvent mixtures (CH_3CN/CH_2Cl_2, CH_3CN/toluene or CH_3CN/EtOAc), although presenting fair to good conversion values even at room temperature as exemplified on entry 3, are undoubtedly less attractive in terms of the development of a green and sustainable approach. In this sense, the use of CH_2Cl_2 is not tolerable nowadays, and it has been detected here that mixtures including toluene or EtOAc give rise to the formation of side products.

The optimal approach (Table 4, entry 8) was extrapolated to the manganese porphyrin catalyst **III** (63.1% of conversion, Table 4, entry 10) and the use of heat was added to conditions previously reported for complex **I** (Table 4, entry 11). Results gathered for

Table 2
Results obtained for the oxidation of substrates 8 and 9 with H_2O_2 catalyzed by the manganese(III) porphyrins (II) and (III)[a].

Substrates	Catalyst	H_2O_2 (m mol)	S/C molar ratio	Conversion (%)	Products selectivity (%)		Time (min)
					S=O	SO_2	
 **(8)**	II	1.8	150	99.7	4.88	95.1	180
		1.8	300	89.3	3.95	96.0	180
	III	1.8	150	96.2	22.1	77.9	180
		1.8	300	72.3	19.9	80.1	180
 **(9)**	II	1.8	150	96.6	73.4	26.6	180
		1.8	300	79.2	80.2	19.8	180
	III	1.8	150	94.1	64.8	35.2	180
		1.8	300	52.7	71.7	28.3	180

[a] The substrate (0.3 mmol) was dissolved in 2.0 mL of CH_3CN and kept under magnetic stirring at 22–25 °C in the presence of Mn-Porph (for S/C molar ratio of 150, the catalyst amount was 2.0×10^{-3} mmol; for S/C molar ratio of 300, the catalyst amount was 1.0×10^{-3} mmol). The co-catalyst used was $NH_4CH_3CO_2$ (0.12 mmol). The oxidant, diluted 1:10 in CH_3CN, was progressively added at regular intervals of 15 min in small aliquots, each corresponding to a half-substrate amount. The conversion and selectivity values are the result of at least two essays.

Table 3
The influence of the S/C molar ratio in the oxidation of thioanisole (**1**) with H_2O_2 catalyzed by (**I**)[a].

S/C molar ratio	H_2O_2 (m mol)	Conversion (%)	Products selectivity (%)		Time (min)
			S=O	SO_2	
300	0.9	99.9	–	100	90
600	0.6	99.9	–	100	60
900	1.8	98.2	–	100	180
1200	1.2	97.2	–	100	120
3000	1.2	96.6	83.5	16.5	120
5000	1.8	86.7	91.3	8.69	180
6000	1.8	62.3	83.0	17.0	180

[a] The substrate (0.3 mmol) was dissolved in 2.0 mL of ethanol and kept under magnetic stirring at 22–25 °C in the presence of the iron(III) catalyst **I**. The oxidant, diluted 1:10 in ethanol, was progressively added at regular intervals of 15 min in small aliquots, each corresponding to a half-substrate amount.

compound **10** when the oxidation in ethanol was performed at 60 °C put in evidence the greater efficiency of $FeTNMe_2F_4PPCl$ (**I**), achieving total conversion (99.9%) and the corresponding sulfone **14** (60.1%) being the major isolated product. It should be mentioned that the blank experiments for compound **10** give rise to conversions lower than 3%. The structures of the sulfoxides and sulfones were confirmed by GC–MS and by ^1H NMR (Supporting information). Because these derivatives afforded suitable single-crystals from crystallization using mixtures of CH_2Cl_2/hexane, the crystal structures of sulfoxides and sulfones **11–16,** not yet reported

Table 4
Results obtained in the optimization of the reaction conditions for 4,6-dimethyldibenzothiophene (**10**) oxidation tests[a].

Entry	Catalyst	S/C molar ratio	Solvent(s)	m (Recovered fractions) (mg)			Conv. (%)
				S.M.	S=O	SO_2	
1[b]	II	150	CH_3CN	31.2	27.8	2.7	56.0
2[b]	II	150	CH_3CN/CH_2Cl_2 (2:1)	41	21.5	17.9	38.0
3[b]	II	300	CH_3CN/CH_2Cl_2 (1:2)	6.6	43.5	16.7	90.0
4[b]	II	300	CH_3CN/toluene (1:2)	22.1	35.8	8.3	66.4
5[b]	II	300	CH_3CN/EtOAc (1:2)	20.3	18.4	24.1	68.6
6[c]	II	150	CH_3CN	13.9	22.2	19.5	78.9
7[d]	II	150	CH_3CN	10.7	17.3	18.0	83.7
8[e]	II	150	CH_3CN	6.3	40.3	24.4	90.5
9[f]	II	150	CH_3CN	7.0	14.4	2.0	89.4
10[e]	III	150	CH_3CN	2.8	13.7	25.2	63.1
11[e]	I	150	EtOH	1.4	4.7	60.1	99.9

Abbreviations: S.M. (starting material); S=O (sulfoxide); SO_2 (sulfone).

[a] Reaction conditions: the catalyst is added (for S/C molar ratio of 150, the catalyst amount was 2.0×10^{-3} mmol; for S/C molar ratio of 300, the catalyst amount was 1.0×10^{-3} mmol) to 0.3 mmol of **10** (64 mg), 0.3 mmol of internal standard (chlorobenzene), and the appropriate volume of solvent until 2.0 mL. With the experiments involving catalysts **II** and **III** it was also necessary to use a co-catalyst, $NH_4CH_3CO_2$ (0.12 mmol). The oxidant (diluted 1:10) was progressively added at regular intervals of 15 min in small aliquots, each corresponding to a half-substrate amount (total amount 1.8 mmol). After 3 h of reaction, with no evolution by TLC, the assays were finished and the reaction mixture purified by preparative TLC.

[b] At r.t. (22–25 °C).

[c] Under sonication.

[d] At 40 °C.

[e] At 60 °C.

[f] At 80 °C.

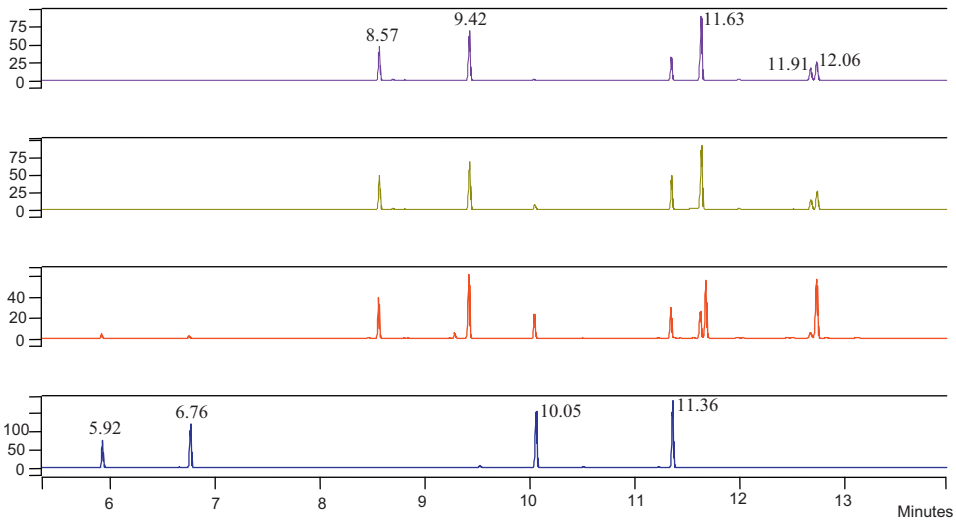


Fig. 5. GC-FID follow-up chromatograms of a model fuel oxidation reaction with H_2O_2 in the presence of catalyst (**I**) for a S/C molar ratio of 150, at room temperature; t_0 initial reaction mixture before the addition of H_2O_2; t_{60} after 60 min of reaction; t_{120} after 120 min of reaction; t_{180} after 180 min of reaction. The model fuel is a solution of **3** (R_t = 5.92), **4** (R_t = 6.76), **8** (R_t = 10.05), and **9** (R_t = 11.36) in hexane (0.03 mmol each). The sulfone of **3** (R_t = 8.57), the sulfone of **4** (R_t = 9.42), the sulfone **12** (R_t = 11.63), the sulfone **16** (R_t = 11.91) and the sulfoxide **15** (R_t = 12.06) are identified in the chromatogram after 180 min of reaction.

in the literature, were also fully elucidated by single-crystal X-ray diffraction studies. The crystal structures of compounds **11** to **16** have been fully elucidated at 150 K using single-crystal X-ray diffraction studies (Fig. 6).[1] All compounds, with the exception of compound **14**, crystallize in either triclinic or monoclinic centrosymmetric space groups with the latter crystallizing instead in the non-centrosymmetric orthorhombic $Pca2_1$ space group. The asymmetric unit of compounds **11** and **12** is composed of two crystallographically independent molecular units (Z' = 2), which result from a combined effect of distinct structural conformations (see Fig. 7 for maximum distances and root mean square distances for the overlay of the two molecules in each compound) and the crystal symmetry of the compound. Noteworthy, in compound **16** the asymmetric unit is solely composed of half of the molecule with the molecular unit depicted in Fig. 6 being, thus, formed by a two-fold crystallographic axis. Individual molecules close pack in the solid state with the aim to effectively fill the available space (not shown). This process is also driven by the presence of a handful of supramolecular interaction, namely weak hydrogen bonding interactions (C—H···O, C—H···S and C—H···p) and p–p contacts.

The excellent catalytic performance of **I** for the sulfoxidation of organosulfur compounds **1–10** prompted us to also evaluate its efficiency in the treatment of refractory *S*-containing compounds on an envisaged model fuel. In this study the model fuel consists of a mixture of benzothiophene (**3**), 3-methylbenzothiophene (**4**), 4-methyldibenzothiophene (**8**) and 4,6-diethyldibenzothiophene (**9**) in hexane and the evolution of the reaction was monitored by GC-FID, being the respective chromatograms at t_0, t_{60}, t_{120}, and t_{180} presented on Fig. 5. After the first oxidant addition the peaks corresponding to substrates **3** (R_t = 5.92), **4** (R_t = 6.76), **8** (R_t = 10.05) and **9** (R_t = 11.36) start to reduce its intensity and the peaks matching the respective oxidation products (namely R_t = 8.57; R_t = 9.42; R_t = 11.63; R_t = 11.91; R_t = 12.06) appear. After 3 h of reaction, more than 80% (84.4%) of the model fuel is converted into the resultant sulfoxides/sulfones. Only the disubstituted DBT **9** (R_t = 11.36) remains in solution.

3. Experimental

3.1. Materials and methods

All solvents and reagents were used as received without further purification. Hydrogen peroxide (30% w/w aqueous solution) was purchased from Riedel-de-Haën and ammonium acetate was supplied by Fluka. The organosulfur compounds (**1–10**) were all purchased from Aldrich.

The GC-FID analyses were performed on a Varian 3900 chromatograph using helium as the carrier gas (30 cm/s). The GC–MS analyses were performed on a Finnigan Trace GC/MS (Thermo Quest

[1] *Crystal data for* **11**: $C_{13}H_{10}OS$, M = 214.27, triclinic, space group $P\bar{1}$, Z = 4, a = 7.6012(11) Å, b = 9.0726(13) Å, c = 15.835(2) Å, α = 92.782(4)°, β = 90.634(4)°, γ = 111.267(4)°, V = 1015.9(3) Å^3, μ(Mo-$K\alpha$) = 0.284 mm^{-1}, D_c = 1.401 g cm^{-3}, colorless blocks, crystal size of 0.08 × 0.08 × 0.06 mm^3. Of a total of 9538 reflections collected, 3713 were independent (R_{int} = 0.0424). Final $R1$ = 0.0493 [$I > 2\sigma(I)$] and $wR2$ = 0.1192 (all data). Data completeness to theta = 25.34°, 99.6%. CCDC 930059.
Crystal data for **12**: $C_{13}H_{10}O_2S$, M = 230.27, triclinic, space group $P\bar{1}$, Z = 4, a = 7.4642(13) Å, b = 10.474(2) Å, c = 13.699(3) Å, α = 92.094(12)°, β = 98.721(11)°, γ = 102.365(11)°, V = 1031.4(3) Å^3, μ(Mo-$K\alpha$) = 0.292 mm^{-1}, D_c = 1.483 g cm^{-3}, colourless plates, crystal size of 0.13 × 0.08 × 0.02 mm^3. Of a total of 16,436 reflections collected, 3719 were independent (R_{int} = 0.1718). Final $R1$ = 0.0815 [$I > 2\sigma(I)$] and $wR2$ = 0.2045 (all data). Data completeness to theta = 25.33°, 99.0%. CCDC 930060.
Crystal data for **13**: $C_{14}H_{12}OS$, M = 228.30, monoclinic, space group $P2_1/n$, Z = 4, a = 7.5731(3) Å, b = 7.6457(3) Å, c = 18.7201(8) Å, β = 91.418(2)°, V = 1083.59(8) Å^3, μ(Mo-$K\alpha$) = 0.271 mm^{-1}, D_c = 1.399 g cm^{-3}, colourless blocks, crystal size of 0.12 × 0.09 × 0.07 mm^3. Of a total of 16,951 reflections collected, 2916 were independent (R_{int} = 0.0262). Final $R1$ = 0.0334 [$I > 2\sigma(I)$] and $wR2$ = 0.0910 (all data). Data completeness to theta = 29.13°, 99.8%. CCDC 930061.
Crystal data for **14**: $C_{14}H_{12}O_2S$, M = 228.30, orthorhombic, space group $Pca2_1$, Z = 4, a = 12.5035(7) Å, b = 7.5528(4) Å, c = 11.9061(6) Å, V = 1124.37(10) Å^3, μ(Mo-$K\alpha$) = 0.272 mm^{-1}, D_c = 1.443 g cm^{-3}, colourless blocks, crystal size of 0.11 × 0.09 × 0.07 mm^3. Of a total of 23,085 reflections collected, 2995 were independent (R_{int} = 0.0258). Final $R1$ = 0.0311 [$I > 2\sigma(I)$] and $wR2$ = 0.0845 (all data). Data completeness to theta = 29.13°, 99.7%. CCDC 930062.
Crystal data for **15**: $C_{16}H_{16}OS$, M = 256.35, monoclinic, space group $P2_1/n$, Z = 4, a = 7.8131(3) Å, b = 21.1480(9) Å, c = 8.4713(4) Å, β = 116.196(2)°, V = 1255.96(9) Å^3, μ(Mo-$K\alpha$) = 0.242 mm^{-1}, D_c = 1.356 g cm^{-3}, colourless plates, crystal size of 0.20 × 0.18 × 0.08 mm^3. Of a total of 13,544 reflections collected, 3372 were independent (R_{int} = 0.0326). Final $R1$ = 0.0371 [$I > 2\sigma(I)$] and $wR2$ = 0.0979 (all data). Data completeness to theta = 29.13°, 99.8%. CCDC 930063.
Crystal data for **16**: $C_{16}H_{16}O_2S$, M = 272.35, monoclinic, space group $C2/c$, Z = 4, a = 14.8197(18) Å, b = 7.6120(8) Å, c = 12.2153(16) Å, β = 110.608(8)°, V = 1289.8(3) Å^3, μ(Mo-$K\alpha$) = 0.245 mm^{-1}, D_c = 1.403 g cm^{-3}, colourless blocks, crystal size of 0.12 × 0.12 × 0.07 mm^3. Of a total of 4141 reflections collected, 1166 were independent (R_{int} = 0.0522). Final $R1$ = 0.0674 [$I > 2\sigma(I)$] and $wR2$ = 0.2312 (all data). Data completeness to theta = 25.34°, 99.1%. CCDC 930064.

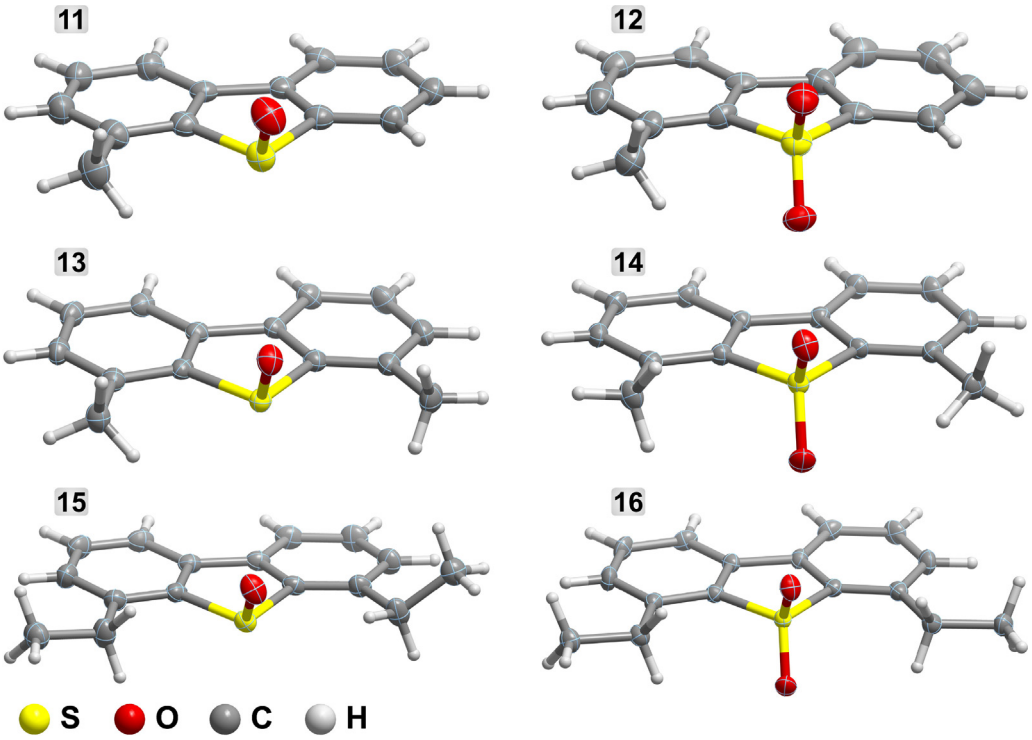


Fig. 6. Schematic representation of the molecular units present in the crystal structures of compounds **11** to **16**. Non-hydrogen atoms are represented as thermal ellipsoids drawn at the 50% probability level and hydrogen atoms as spheres with arbitrary radii.

CE instruments) using helium as the carrier gas (35 cm/s). In both cases fused silica capillary DB-5 type columns (30 m, 0.25 mm i.d., 0.25 μm film thickness) were used. The ^{1}H NMR spectra were recorded on a Bruker Avance 300 at 300.13 MHz, using $CDCl_3$ as solvent and TMS as the internal reference.

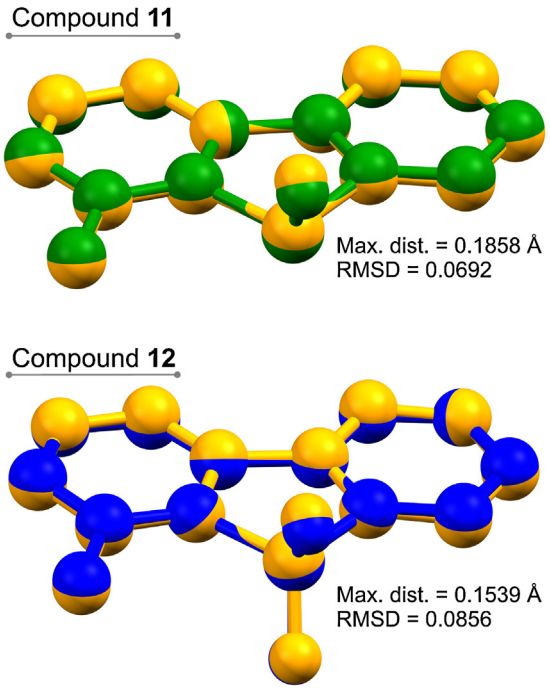


Fig. 7. Overlay of the two crystallographically independent molecular units composing the asymmetric unit of compounds **11** and **12** (Z' = 2). For clarity, hydrogen atoms have been omitted and each molecule is represented in a different color. Molecular overlay performed using the software package Mercury. [56].

3.2. Homogeneous catalysis with MPorph (M = Fe, Mn)

All the MPorph catalysts were synthesized according to well-established procedures in our laboratory [46]. Generally, for the homogeneous catalytic assays with substrates **1–9**, the substrate (0.3 mmol), the catalyst (2.0×10^{-3} mmol; 1.0×10^{-3} mmol; 0.5×10^{-3} mmol, depending on the S/C molar ratio employed: 150; 300; 600, respectively), and the internal standard (0.3 mmol) were dissolved in 2.0 mL of the appropriate solvent (ethanol for the iron complex **I**, and CH_3CN for the manganese complexes **II** and **III**). Conversely in the experiments with catalyst **I**, where no co-catalyst is needed, with the manganese catalysts (**II** and **III**) ammonium acetate (0.12 mmol) was used as co-catalyst. The reaction mixtures were kept under magnetic stirring, in the absence of light, and at 22–25 °C. The oxidant [H_2O_2 30% (w/w) aqueous solution] was diluted (1:10) in the suitable solvent (ethanol for **I**, and CH_3CN for **II** and **III**) and progressively added to the reactions in aliquots corresponding to half of the substrate amount. All the experiments were followed by GC-FID and were stopped when, after two successive oxidant additions, no significant changes on the conversion of the substrate and on the sulfoxide/sulfone ratio were observed.

For the 4,6-DMDBT (**10**), since it is insoluble in pure CH_3CN or ethanol at room temperature, some modifications to the aforementioned protocol were introduced. Thus, in order to increase substrate solubility, the catalytic experiments were performed with several mixtures of solvents or at higher temperature. For the optimal conditions, the established temperature was 60 °C and the reactions were followed by TLC. After 3 h of reaction (with no evolution observed by TLC) the reactions were finished, the reaction mixtures were applied on preparative TLC plates, and 3 fractions were isolated using a mixture of CH_2Cl_2/petroleum ether (1:2) as eluent. The starting material (S.M.) and the fractions corresponding to the oxidation products, the sulfoxide (S=O) and the sulfone (SO_2), were recovered, crystallized using a mixture of hexane/CH_2Cl_2 (2:1), weighed, and characterized by ^{1}H NMR (Supporting information) and single-crystal X-ray diffraction.

3.3. Model fuel oxidation

For the experiments with the model fuel, the most efficient iron(III) catalyst (**I**) was chosen, and all the assays, as in the previous catalytic tests, were performed at room temperature in the absence of light. Thus, the catalyst (8.0×10^{-3} mol in 570 μL of ethanol) was added to the four organosulfur compounds **3**, **4**, **8**, **9** (0.03 mmol each) dissolved in hexane, for a total volume of 2.0 mL. The oxidant (30% aqueous H_2O_2) diluted in ethanol (1:10) was progressively added to the reaction mixture in small aliquots, each corresponding to 0.5 eq. at every 15 min. The reaction was monitored by GC-FID and stopped when no evolution occurred after two sucessive analyses.

3.4. Single-crystal X-ray diffraction studies

Suitable single-crystals of compounds **11** to **16** were manually harvested directly from the crystallization vials and mounted on Hampton Research CryoLoops using FOMBLIN Y perfluoropolyether vacuum oil (LVAC 25/6) purchased from Sigma-Aldrich [47] with the help of a Stemi 2000 stereomicroscope equipped with Carl Zeiss lenses. Data were collected at 150(2) K on a Bruker X8 Kappa APEX II charge-coupled device (CCD) area-detector diffractometer (Mo-*K*α graphite-monochromated radiation, λ = 0.71073 Å) controlled by the APEX2 software package [48], and equipped with an Oxford Cryosystems Series 700 cryostream monitored remotely using the software interface Cryopad [49]. Images were processed using the software package SAINT+ [50], and data were corrected for absorption by the multi-scan semi-empirical method implemented in SADABS [51]. Structure were solved by the direct methods of SHELXS-97 [52,53], and refined by full-matrix least squares on F^2 using SHELXL-97 [52,54]. All non-hydrogen atoms were directly located from difference Fourier maps and successfully refined with anisotropic displacement parameters.

Hydrogen atoms bound to carbon were placed at their idealized positions using appropriate *HFIX* instructions in SHELXL (43 for the aromatic groups, 23 for the methylene and 137 for the methyl groups) and included in subsequent least-squares refinements with an isotropic displacement parameter (U_{iso}) fixed at 1.2 (for the aromatic and —CH_2— hydrogen atoms) or 1.5 (for the —CH_3 group) of U_{eq} of the parent carbon atom.

The last difference Fourier map synthesis showed: for **11**, the highest peak (0.578 eÅ^{-3}) and deepest hole (−0.381 eÅ^{-3}) located at 0.94 and 0.71 Å from S2, respectively; for **12**, the highest peak (0.394 eÅ^{-3}) and deepest hole (−0.364 eÅ^{-3}) located at 0.82 and 0.95 Å from C14 and S1, respectively; for **13**, the highest peak (0.384 eÅ^{-3}) and deepest hole (−0.236 eÅ^{-3}) located at 0.81 and 0.55 Å from C14 and S1, respectively; for **14**, the highest peak (0.400 eÅ^{-3}) and deepest hole (−0.249 eÅ^{-3}) located at 0.70 and 1.29 Å from C8 and C14, respectively; for **15**, the highest peak (0.349 eÅ^{-3}) and deepest hole (−0.288 eÅ^{-3}) located at 0.69 and 0.56 Å from C12 and S1, respectively; for **16**, the highest peak (1.096 eÅ^{-3}) and deepest hole (−0.599 eÅ^{-3}) located at 0.90 and 1.62 Å from C7 and H_3, respectively. Structural drawings have been produced using the software package Crystal Diamond [55].

4. Conclusions

Herein we present an efficient and environmentally friendly approach, involving the use of an iron(III) porphyrin complex as catalyst and aqueous hydrogen peroxide as oxidant, promoting the oxidation of several organosulfur compounds, including the so-called *S*-refractory compounds (BTs and DBTs). Comparatively to the previously described procedure described by us using the manganese(III) catalysts **II** and **III**, the iron catalyst **I** demonstrates higher efficiency, allowing excellent conversions, faster reactions, and the use of smaller amounts of catalyst. When using a S/C molar ratio of 1200, it was possible to observe a major drop on the conversion values, mainly for substrates **4**, **6** and **9**; even when using a S/C molar ratio of 600, conversions are still between 88.6% and 99.9%. Furthermore, catalyst **I** is the only one able to promote the total conversion of substrate **10**, mainly to the corresponding sulfone **14** (92.7% selectivity). The use of ethanol in the catalytic assays with porphyrin **I** as a green solvent also meets the present policies of sustainable chemistry promoting the development of increasingly cleaner procedures [29].

Trying to envisage the potential application of metalloporphyrin based catalysts in an ODS methodology, catalyst **I** was also successfully evaluated in the oxidation of a model fuel (mixture of substrates **3**, **4**, **8**, **9** in hexane). After 3 h of reaction the major part of the model fuel was oxidized, remaining in solution only a small amount of substrate **9**. Despite that, the high potential of porphyrin complexes as catalysts for the sulfoxidation of the *S*-refractory benzothiophenes and dibenzothiophenes by H_2O_2 was demonstrated.

Acknowledgments

We would like to thank Fundação para a Ciência e a Tecnologia (FCT, Portugal), the European Union, QREN, FEDER, COMPETE, for funding the Organic Chemistry Research Unit (QOPNA) (PEst-C/QUI/UI0062/2013) and CICECO (PEst-C/CTM/LA0011/2013). Authors also acknowledge the Portuguese National NMR Network, supported with funds from FCT. S.L.H. Rebelo thanks project NORTE-07-0124-FEDER-000067-nanochemistry for her grant. S.M.G. Pires also thanks FCT for her PhD Grant (SFRH/BD/64354/2009) and F.A.A. Paz would like to thank FCT for the financial support towards the purchase of the single-crystal diffractometer.

Appendix A. Supplementary data

Supplementary data associated with this article can be found, in the online version, at http://dx.doi.org/10.1016/j.apcatb.2014.05.003.

References

[1] X. Ma, A. Zhou, C. Song, Catal. Today 123 (2007) 276–284 (and references cited therein).
[2] F. Al-Shahrani, T. Xiao, S.A. Llewellyn, S. Barri, Z. Jiang, H. Shi, G. Martinie, M.L.H. Green, Appl. Catal., B: Environ. 73 (2007) 311–316 (and references cited therein).
[3] J.M. Campos-Martin, M.C. Capel-Sanchez, P. Peres-Presas, J.L.G. Fierro, J. Chem. Technol. Biotechnol. 85 (2010) 879–890 (and references cited therein).
[4] R. Gatan, P. Barger, V. Gembicki, Prepr. Pap.—Am. Chem. Soc., Div. Fuel Chem. 49 (2004) 577–579.
[5] M. Soleimani, A. Bassi, A. Margaritis, Biotechnol. Adv. 25 (2007) 570–596.
[6] B. Pawelec, R.M. Navarro, J.M. Campos-Martin, J.L.G. Fierro, Catal. Sci. Technol. 1 (2011) 23–42.
[7] R.T. Bachmann, A.C. Johnson, R.G.J. Edyvean, Int. Biodeterior. Biodegrad. 86 (2014) 225–237.
[8] J. Zongxuan, L. Hongying, Z. Yongna, L. Can, Chin. J. Catal. 32 (2011) 707–715.
[9] Y. Wang, G. Li, X. Wang, C. Jin, Energy Fuels 21 (2007) 1415–1419.
[10] K. Ryu, J. Kim, J. Heo, Y. Chae, Biotechnol. Lett. 24 (2002) 1535–1538.
[11] L.C. Caero, E. Hernandez, F. Pedraza, F. Murrieta, Catal. Today 107 (2005) 564–569 (and references cited therein).
[12] R. Villar, I. Encio, M. Migliaccio, M.J. Gil, V. Martinez-Merino, Bioorg. Med. Chem. 12 (2004) 963–968.
[13] R. Bentley, Chem. Soc. Rev. 34 (2005) 609–624 (and references cited therein).
[14] K. Kamata, T. Hirano, R. Ishimoto, N. Mizuno, Dalton Trans. 39 (2010) 5509–5518 (and references cited therein).
[15] I. Fernández, N. Khiar, Chem. Rev. 103 (2003) 3651–3705.
[16] J.T. Groves, in: P.R. Ortiz de Montellano (Ed.), Cytochrome P-450: Structure, Mechanism, and Biochemistry, third ed., Kluwer Academic/Plenum Publishers, New York, NY, 2005 (Chapter 1).
[17] W. Lohmann, U. Karst, Anal. Bioanal. Chem. 391 (2008) 79–96.
[18] F.P. Guengerich, C.D. Sohl, G. Chowdhury, Arch. Biochem. Biophys. 507 (2011) 126–134.

[19] S. Rendic, F.P. Guengerich, Chem. Res. Toxicol. 25 (2012) 1316–1383.
[20] J.T. Groves, T.E. Nemo, R.S. Myers, J. Am. Chem. Soc. 101 (1979) 1032–1033.
[21] K.S. Suslick, in: K. Kadish, K. Smith, R. Guillard (Eds.), The Porphyrin Handbook, Academic Press, New York, NY, 1999.
[22] C. Che, J. Huang, Chem. Commun. (2009) 3996–4015.
[23] D. Mansuy, C.R. Chimie 10 (2007) 392–413.
[24] A. Rezaeifard, M. Jafarpour, P. Farshid, A. Naeimi, Eur. J. Inorg. Chem. (2012) 5515–5524.
[25] E. Brulé, Y.R. de Miguel, Org. Biomol. Chem. 4 (2006) 599–609.
[26] S.M.G. Pires, M.M.Q. Simões, I.C.M.S. Santos, S.L.H. Rebelo, M.M. Pereira, M.G.P.M.S. Neves, J.A.S. Cavaleiro, Appl. Catal., A: Gen. 439–440 (2012) 51–56.
[27] S.L.H. Rebelo, M.M. Pereira, M.M.Q. Simões, M.G.P.M.S. Neves, J.A.S. Cavaleiro, J. Catal. 234 (2005) 76–87.
[28] S. Zakavi, A. Abasi, A.R. Pourali, S. Talebzadeh, Bull. Korean Chem. Soc. 33 (2012) 35–38.
[29] R.A. Sheldon, Chem. Soc. Rev. 41 (2012) 1437–1451.
[30] K. Alfonsi, J. Collberg, P.J. Dunn, T. Fevig, S. Jennings, T.A. Johnson, H.P. Kleine, C. Knight, M.A. Nagy, D.A. Perry, M. Stefaniak, Green Chem. 10 (2008) 31–36.
[31] E. Baciocchi, M.F. Gerini, A. Lapi, J. Org. Chem. 69 (2004) 3586–3589.
[32] P. Le Maux, G. Simonneaux, Chem. Commun. 47 (2011) 6957–6959.
[33] X. Zhou, S. Lv, H. Wang, X. Wang, J. Liu, Appl. Catal., A: Gen. 396 (2011) 101–106.
[34] S.M.G. Pires, R. De Paula, M.M.Q. Simões, M.G.P.M.S. Neves, I.C.M.S. Santos, A.C. Tomé, J.A.S. Cavaleiro, Catal. Commun. 11 (2009) 24–28.
[35] S.L.H. Rebelo, M.M.Q. Simões, M.G.P.M.S. Neves, J.A.S. Cavaleiro, J. Mol. Catal. A: Chem. 201 (2003) 9–22.
[36] S.L.H. Rebelo, M.M.Q. Simões, M.G.P.M.S. Neves, A.M.S. Silva, P. Tagliatesta, J.A.S. Cavaleiro, J. Mol. Catal. A: Chem. 232 (2005) 135–142.
[37] P. Tagliatesta, D. Giovannetti, A. Leoni, M.G.P.M.S. Neves, J.A.S. Cavaleiro, J. Mol. Catal. A: Chem. 252 (2006) 96–102.
[38] S.M.G. Pires, R. De Paula, M.M.Q. Simões, A.M.S. Silva, M.R.M. Domingues, I.C.M.S. Santos, M.D. Vargas, V.F. Ferreira, M.G.P.M.S. Neves, J.A.S. Cavaleiro, RSC Adv. 1 (2011) 1195–1199.
[39] S.L.H. Rebelo, M.M.Q. Simões, M.G.P.M.S. Neves, A.M.S. Silva, J.A.S. Cavaleiro, A.F. Peixoto, M.M. Pereira, M.R. Silva, J.A. Paixão, A.M. Beja, Eur. J. Org. Chem. (2004) 4778–4787.
[40] C.M.B. Neves, M.M.Q. Simões, I.C.M.S. Santos, F.M.J. Domingues, M.G.P.M.S. Neves, F.A.A. Paz, A.M.S. Silva, J.A.S. Cavaleiro, Tetrahedron Lett. 52 (2011) 2898–2902.
[41] C.M.B. Neves, M.M.Q. Simões, M.R.M. Domingues, I.C.M.S. Santos, M.G.P.M.S. Neves, F.A.A. Paz, A.M.S. Silva, J.A.S. Cavaleiro, RSC Adv. 2 (2012) 7427–7438.
[42] M.M.Q. Simões, R. De Paula, M.G.P.M.S. Neves, J.A.S. Cavaleiro, J. Porphyrins Phthalocyanines 13 (2009) 589–596.
[43] M.M.Q. Simões, C.M.B.S. Neves, M.G. Pires, M.G.P.M.S. Neves, J.A.S. Cavaleiro, Pure Appl. Chem. 85 (2013) 1671–1681.
[44] N.A. Stephenson, A.T. Bell, J. Mol. Catal. A: Chem. 275 (2007) 54–62.
[45] A. Thellend, P. Battioni, D. Mansuy, J. Chem. Soc., Chem. Commun. (1994) 1035–1036.
[46] (a) R. De Paula, M.A.F. Faustino, D.C.G.A. Pinto, M.G.P.M.S. Neves, J.A.S. Cavaleiro, J. Heterocycl. Chem. 45 (2008) 453–459;
(b) A.D. Adler, F.R. Longo, F. Kampas, J. Kim, J. Inorg. Nucl. Chem. 32 (1970) 2443–2445.
[47] T. Kottke, D. Stalke, J. Appl. Crystallogr. 26 (1993) 615–619.
[48] APEX2, Data Collection Software Version 2.1-RC13, Bruker AXS, Delft, The Netherlands, 2006.
[49] Cryopad, Remote Monitoring and Control, Version 1.451, Oxford Cryosystems, Oxford, United Kingdom, 2006.
[50] SAINT+, Data Integration Engine v. 7.23a©, Bruker AXS, Madison, WI, USA, 1997–2005.
[51] G.M. Sheldrick, SADABS v.2.01, Bruker/Siemens Area Detector Absorption Correction Program, Bruker AXS, Madison, WI, USA, 1998.
[52] G.M. Sheldrick, Acta Crystallogr., Sect. A: Found. Crystallogr. 64 (2008) 112–122.
[53] G.M. Sheldrick, SHELXS-97, Program for Crystal Structure Solution, University of Göttingen, 1997.
[54] G.M. Sheldrick, SHELXL-97, Program for Crystal Structure Refinement, University of Göttingen, 1997.
[55] K. Brandenburg, DIAMOND, Version 3.2f, Crystal Impact GbR, Bonn, Germany, 1997–2010.
[56] I.J. Bruno, J.C. Cole, P.R. Edgington, M. Kessler, C.F. Macrae, P. McCabe, J. Pearson, R. Taylor, Acta Crystallogr., Sect. B: Struct. Sci. 58 (2002) 389–397.